

# Wrinkle generation mechanism during draw bending forming

†\*Xia Zhu<sup>1</sup>, Keiji Ogi<sup>1</sup> and Nagatoshi Okabe<sup>1</sup>

<sup>1</sup>Department of Mechanical Engineering, Faculty of Engineering, Ehime University, JP

\*Presenting author: zhu.xia.mx@ehime-u.ac.jp

†Corresponding author: zhu.xia.mx@ehime-u.ac.jp

## Abstract

The purpose of this research is to focus on wrinkles, which are the main processing limit factor of draw bending, and to elucidate the mechanism of the generation. The forming experiments provided data for verifying the validity of the analytical model and the limits of crease formation. In addition, the effect of the friction coefficient between the pipe and the bending die on the occurrence of wrinkles was confirmed by finite element analyses. Furthermore, by analyzing the deformation behavior inside the material during the draw bending process, the mechanism of the wrinkle was clarified. The following findings were obtained from this study. First, wrinkles occur not at the bend but at the straight pipe part on the raw pipe side. Next, the coefficient of friction between the pipe and the bending die promotes wrinkles and the growth of the generated wrinkles. Finally, the wrinkles are formed by the transition of the flexure due to the drawing-rolling phenomenon in the draw bending forming.

**Keywords:** Draw bending forming, Wrinkles, Finite-element method

## Introduction

Metal pipes, such as plumbing, have been used for fluid transportation for a long time and form a transportation path together with fittings, such as elbows, within the structure. However, in view of the demands for energy saving and cost reduction in recent years, reduction of joints and thinning of pipes are required. Therefore, a method has been adopted in which the pipe is processed by draw bending processing, and the number of joints used is suppressed by forming a bent portion at an arbitrary position [1-5]. Here, when the wall thickness of the pipe becomes thin, problems such as high flattening rate, wrinkles, and plastic buckling occur. A wrinkle is considered undesirable except for special processing, such as wrinkle bending, and the wrinkle is classified as defective at the stage of wrinkle generation. Compared to plastic buckling, wrinkles are more likely to occur, which is a major factor in the processing limit of rotary drawing and bending.

The purpose of this research is to determine the state inside the material using finite-element analysis and to improve the performance of draw bending forming by clarifying the mechanism of wrinkle generation. An analytical model of rotational drawing was made by using the general-purpose nonlinear finite-element analysis software MSC Marc 2016, and the analytical results were compared with experimental results to verify the validity of the model. Furthermore, the mechanism of wrinkle generation was investigated.

## Verification of analytical model validity

Fig. 1 shows a process schematic view of the draw bending process. Here,  $R$  is the bending radius of a bending die,  $\omega$  is the rotational speed of a bending die, and  $\theta$  is the bending angle of a bending die. Prior to investigating the mechanism of wrinkle generation, the validity of the analytical model was verified. In this study, plastic deformation behaviors of the material and the friction coefficient between the pipe and the bending die were focused on as parameters

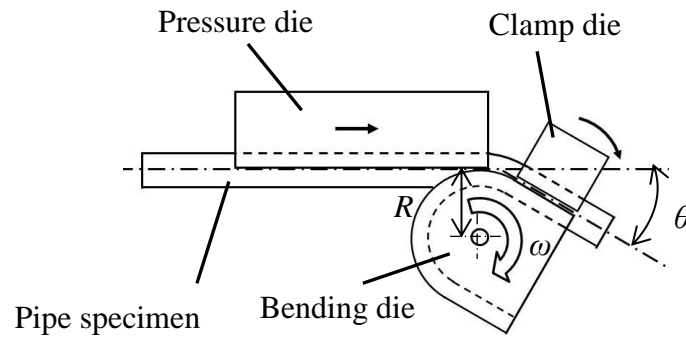


**Fig. 1 Schematic diagram of draw bending forming**

**Table 1 Numbers of element and minimum element size**

	Numbers of elements	Minimum element size
Axial direction	65 (Bend part divided in half again)	1 mm
Circumferential direction	18	0.698 mm ( $10^\circ$ )
Radial direction (thickness)	6	0.1667 mm

affecting the wrinkles generated during the draw bending forming.

Under the processing conditions in which no wrinkling occurs, the influence of the friction coefficient is smaller to the plastic deformation behavior. Therefore, the frictional force generated between the pipe and bending die is small under the processing condition in which wrinkles do not occur, even in actual processing. Therefore, to verify the validity of the material properties used for the analysis, the flattening ratio  $f = (D_{\max} - D_{\min}) / D_0$  of the bent portion of the pipe specimen after processing was investigated under the processing condition in which wrinkles do not occur. Here,  $D_{\max}$ ,  $D_{\min}$ ,  $D_0$  are the major axis, minor axis, and outer diameter of the original pipe in the cross section of the bent portion.

#### *Experimental conditions*

A SUS 304 (Japanese Industrial Standards, JIS G 3448 : 2012) seamless steel pipe with an outside diameter  $D_0 = 10$  mm, which is widely used for pipes, was used, with a wall thickness  $t_0 = 1.0$  mm. A bending radius  $R$  of the bending die was fixed at 20 mm, the rotational angular velocity  $\omega$  was fixed at 120 rpm, the bending angle  $\theta$  was changed from  $15^\circ$  to  $120^\circ$  at intervals of  $15^\circ$ , and processing experiments were conducted.

#### *Analytical conditions*

As shown in Fig. 1, a bending die, a clamping die, and a pressure die were defined as rigid bodies, and the pipe was defined as an elastoplastic body with twenty-node three-dimensional isoparametric elements in the analytical model. In consideration of symmetry, a 1/2 model was used.  $D_0$  and  $t_0$  are identical to the experimental conditions, and the axial length is 130 mm. Table 1 shows numbers of element and the minimum mesh size. An ideal condition was set

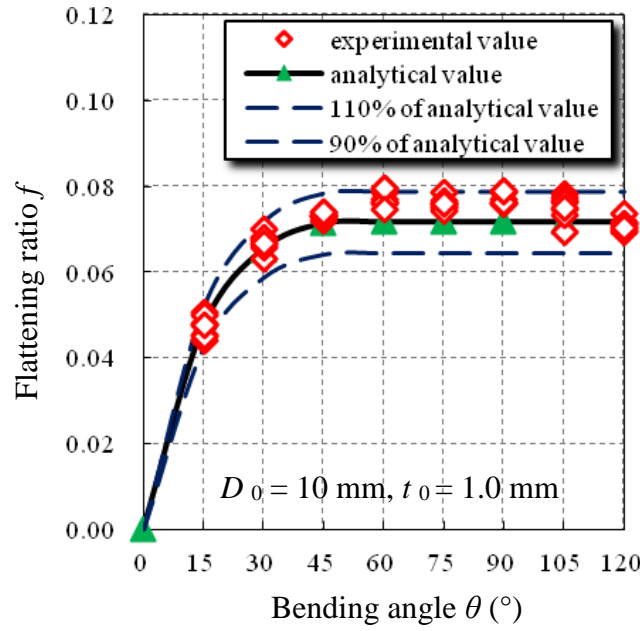


**Fig. 2 Comparison of flattening ratio for experiment and analysis results**

when the coefficient of friction  $\mu$  between the pipe and the bending dice was 0.0. Young's modulus  $E = 193$  GPa, Poisson's ratio  $\nu = 0.29$ , and yield stress  $\sigma_y = 320$  MPa were used as material properties. For the plastic deformation behavior, the relationship between the true stress  $\sigma$  and the true strain  $\varepsilon$  in the plastic region is shown in Eq. 1, and an approximation formula of the Ludwik type [6] is used.

$$\sigma = \sigma_y + K_p (\varepsilon - \varepsilon_y)^n \quad (1)$$

Where  $\varepsilon_y$  is the yield strain,  $K_p$ , and  $n$  is the material constant. In this study,  $K_p = 1600$  MPa and  $n = 0.85$  were used.

#### *Evaluation of the validity of the analytical model*

Figure 2 shows flattening ratios  $f$  obtained by experiments and analyses. Increments of  $\pm 10\%$  of the analysis value are indicated by a broken line. It is suggested that the average value of the experimental results is within  $\pm 10\%$  of the analysis results. From the Fig.2, it is judged that the analysis model can sufficiently reproduce the draw bending process. Therefore, this analytical model was used in examining the wrinkle occurrence mechanism to be described later.

### **Investigation on mechanism of wrinkles**

#### *Criterion for wrinkles*

Wrinkles are believed to be due to buckling that occurs on the inside (the compression side) of the bend. However, in the actual bending process, shear stress, axial force, etc. are added to the bending moment, and in the rotational pull bending process, the machined part changes dynamically as the piping material is drawn into the bending die as the process progresses. Here, we focused on the borderline of wrinkle. Table 2 shows the dimensions of the pipe specimens and bending dice. In addition to the conditions in Table 2, experiments were conducted with  $\omega = 7000$  ° / min and  $\theta = 120$  °, and the occurrence of wrinkles at the bend was investigated by

**Table 2 Dimensions of the pipe specimens and bending dies**

Initial outer diameter $D_0$ (mm)	Initial thickness $t_0$ (mm)	Bending radius $R$ (mm)
10	0.5, 0.8, 1.0, 1.2	15, 20, 25
14	0.5, 0.8, 1.0, 1.2, 1.5	20, 28, 35

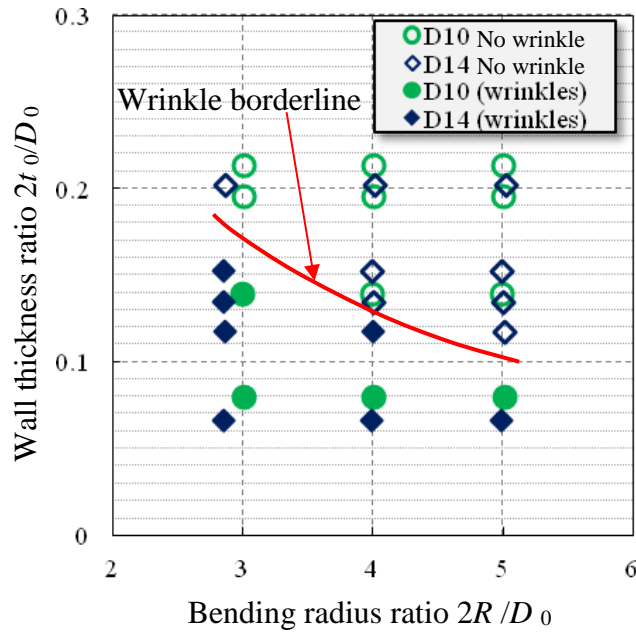


**Fig. 3 Wrinkle borderline**

the forming experiments. Figure 3 shows the bending radius ratio  $2R/D_0$  and the thickness ratio  $2t_0/D_0$  in which the bending radius  $R$  and the thickness  $t_0$  are made nondimensional by the radius  $D_0/2$  of the piping material, respectively. The experimental conditions where wrinkles did not occur are indicated by hollow markers, and the experimental conditions where wrinkles occurred are indicated by solid markers, a boundaries of wrinkles in this experiment are shown by solid lines in the figure. From Fig.3, even if the dimensions of the material and the bending die are different, if the ratio of  $D_0$ ,  $t_0$  and  $R$  is the same, the wrinkle borderline is the same.

On the other hand, simulation analysis was performed on a thin-walled pipe with  $D_0 = 10$  mm,  $t_0 = 0.5$  mm ( $2R/D_0 = 4.0$ ,  $2t_0/D_0 = 0.1$ ,  $R = 20$  mm), and an example of the result is shown in Fig. 4. As the forming process progressed, wrinkles were generated not from the bend of the pipe but from the straight pipe part on the raw pipe side. This was the same even at the stage where the first wrinkle occurred under the same conditions. Therefore, it was found that wrinkles were generated not at the bend but at the straight pipe section on the base pipe side.

#### *Effect of friction coefficient on wrinkles*

The borderline of the presence or absence of wrinkles was investigated by FEM analysis assuming that the coefficient of friction  $\mu = 0, 2.0$ , and is shown by the broken line in Fig.5. The borderline of  $\mu = 2.0$  is almost in agreement with the experimental result shown by the solid

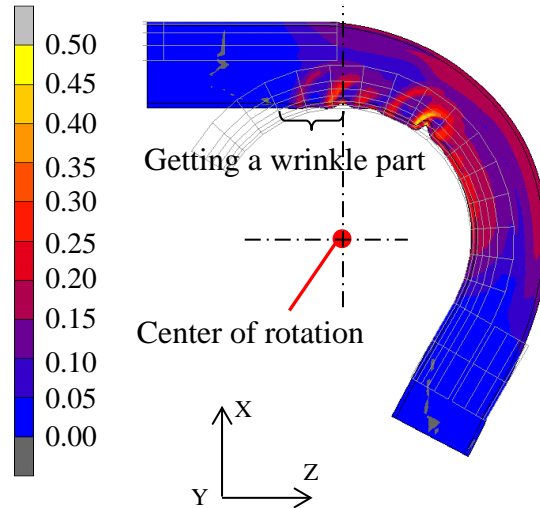


Fig. 4. Equivalent plastic strain contour ( $D_0 = 10 \text{ mm}$ ,  $t_0 = 0.5 \text{ mm}$ ).

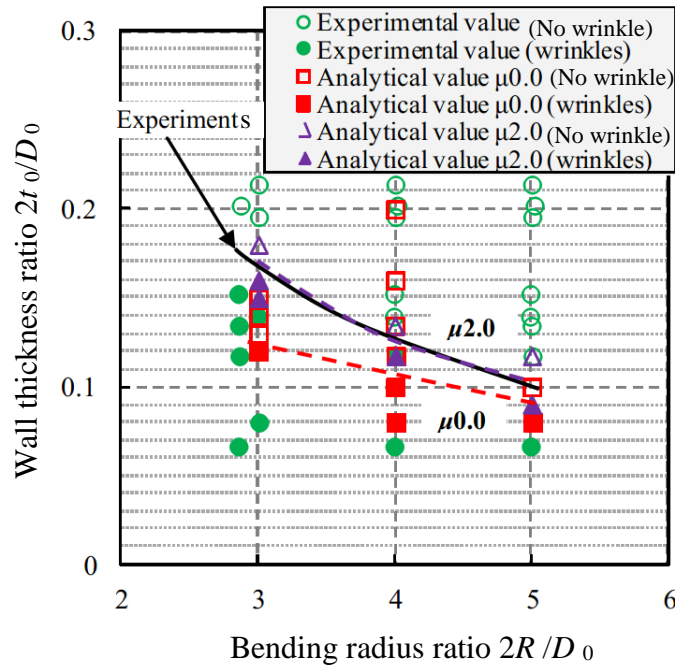
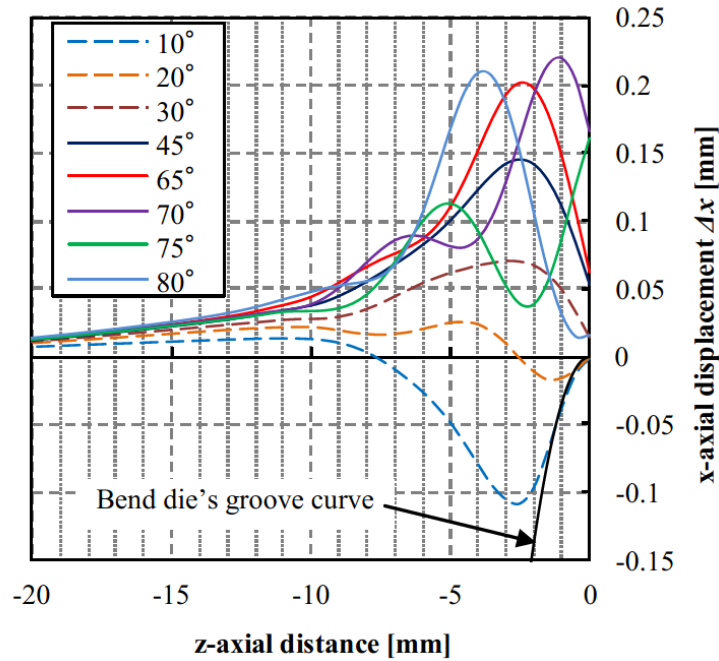


Fig.5 Comparison of borderline curves for initiation of wrinkles

line. The smaller the value of  $\mu$ , the lower the crease of creases, and the less the creases become. In addition, the smaller the bending radius of the bending die, the more sensitive the borderline of crease formation to friction, and the more it changes with the size of the coefficient of friction.

#### Mechanism of wrinkles

This study has clarified that the wrinkles occur not inside the bend but inside the straight pipe. Therefore, using the contact point between the pipe and the bending die at  $\theta = 0^\circ$  as the reference point, the displacement  $\Delta x$  of the bending inner surface of the pipe in the x-axis direction (see Fig. 4) was investigated from the reference point to the base pipe side. Fig. 6 shows the x-axis displacement  $\Delta x$  for each bending angle at  $D_0 = 14 \text{ mm}$ ,  $t_0 = 0.5 \text{ mm}$ ,  $R = 28$



**Fig.6 x-axial displacement ( $2 R / D_0 = 4.0$ ,  $2 t_0 / D_0 = 0.1$ ,  $\mu = 2.0$ )**

mm ( $2 R / D_0 = 4.0$ ,  $2 t_0 / D_0 = 0.071$ ), and  $\mu = 2.0$  obtained by analysis. The broken line is  $\Delta x$  at the stage where wrinkles have not occurred.

Immediately after the start of bending, deformation caused by the Hertzian contact occurred, which is also referred to as the drawing-rolling phenomenon, in the draw bending processing. The deflection to the side of the bending die due to the drawing-rolling phenomenon changes with the progress of processing, becomes maximum around the bending angle  $\theta = 10^\circ$  to  $15^\circ$ , and then decreases. Furthermore, with the increase of the bending angle  $\theta$ , the deformed portion due to the drawing-rolling phenomenon is made uniform by the contact with the bending die, and the straight pipe portion on the raw pipe side begins to bend outward on the opposite side of the bending die.

The deflection converges to a constant value under processing conditions where wrinkles do not occur. On the other hand, under the processing conditions where wrinkles occurred, the deflection continued to increase and eventually became wrinkles. In addition, in this study, it was confirmed that wrinkles occurred in the region from the flexible portion to the straight pipe portion, which was slightly deviated from the maximum flexible portion, but not from the maximum flexible portion.

In the experiment, wrinkles occurred, but in the analysis of  $\mu = 0.0$ , deformation similar to that in the case of wrinkles was observed even under processing conditions in which no wrinkles occurred. However, under this condition, the deformation was equalized by the bending die as the processing progressed, and no wrinkles were finally confirmed. From these facts, it was found that the wrinkles are formed by the transition of the flexure due to the drawing-rolling phenomenon.

## Conclusions

The following findings were obtained from this study.

Wrinkles occur not at the bend but at the straight pipe part on the raw pipe side.

The coefficient of friction between the pipe and the bending die promotes the occurrence of wrinkles and the growth of the generated wrinkles.

The deflection of piping starting from the drawing-rolling phenomenon converges to a constant value in the processing condition where wrinkles do not occur.

Wrinkles are formed by the transition of flexures due to the drawing-rolling phenomenon in rotary bending.

## References

- [1] The Japan Plastic Processing Society, *Tube Forming – Secondary Processing of Tubular Materials and Product Design* –, Corona Company, Tokyo, 1992, pp. 39 – 40.
- [2] Shigeki Mori, Ken-ichi Manabe, Hisashi Nishimura and Kimio Tamura, Deformation of Clad Tubes in Rotary Draw Bending, *J. of JSTP*, **33**–378 (1992) 862 – 867.
- [3] Osamu Sonobe, Yuji Hashimoto, Koji Suzuki, Kei Sakata and Ken-ichi Kawai, Experimental and Analytical Studies of Deformation Behavior of ERW Tubes in Rotary Draw Bending, *J. of JSTP*, **51** – 589 (2010) 121 – 125.
- [4] Shuji Sakaki, Yusuke Okude and Shoichiro Yoshihara, Working Limit for Several Types of Cross Section in Draw Bending, *J. of JSTP*, **53** – 614 (2012) 246 – 250.
- [5] Masabumi Yuhara, Makoto Hoshino and Osamu Wada, Draw Bending of Tube Using Ultrasonic-Vibration Plug, *J. of JSTP*, **53** – 618 (2012) 646 – 650.
- [6] Fusahito Yoshida, *Foundations of Elastic Plastic Dynamics*, First edition, 12 press, Kyoritsu Publishing, Tokyo, 2008, p. 116.